

## Methods of Preventing the Spread of Zinc Contamination During Vacuum Processing

Paul S. Korinko, Savannah River National Laboratory, Materials Science and Technology, Aiken, SC

Andrew J. Duncan, Savannah River National Laboratory, Materials Science and Technology, Aiken, SC

Kevin J. Stoner, Savannah River Tritium Enterprise, Aiken, SC

### Abstract

Radioactive zinc,  $^{65}\text{Zn}$ , was detected after a thermal vacuum process that extracted a desired product from articles out of a commercial light water reactor. While the facility is designed to handle radioactive materials, the location of the  $^{65}\text{Zn}$  was in an area that is not designed for gamma emitting contaminants. A series of experiments were conducted to entrain the contaminant in an easily replaceable trap within the process piping. The experiments were conducted with increasing levels of complexity. Initially a simple apparatus was developed to determine the effect of substrate temperature on the vapor capture, this was followed by experiments to determine the effect of filter pore size on pumping and trapping, finally the interactive effects of both pore size and temperature were evaluated. The testing was conducted on a system that used a roughing vacuum pump using model and prototypic materials. It was determined that heating the substrate to nominally 200°C resulted in effective trapping on the model as well as prototypic material.

### Introduction

Gamma emitting contamination of  $^{65}\text{Zn}$  deposits were detected in a vacuum pumping system after a thermal treatment of irradiated objects (1). Select deposits were analyzed and it was determined that the source of the contamination was vapor deposition of small amounts of activated zinc from residual elements in the irradiated objects. The deposits were characterized and for shape and adhesion as described in Reference 1.

A review of vapor deposition literature reveals that the deposition morphology is dependent on the gas saturation, the deposition temperature, and the presence of impurity gas species (2). Physical vapor deposition has been used to deposit both coatings and to make particles for over 40 years. Airco-Temescal (3) indicates that surface roughness, shape composition and cleanliness also affect the deposition morphology. It is further indicated that at substrate temperatures of nominally 10% the homologous temperature ( $T/T_{m(\text{abs})} = T_H$ ) particles rather than a deposit will be formed, at 30%  $T_H$  a columnar, though porous, structure is formed, at 60%  $T_H$  it becomes equiaxed, and at 80%  $T_H$  epitaxial structures are possible. This zone definition for the zone descriptions is shown schematically in Figure 1 (5). Other researchers (6, 7, 8 & 9) describe the formation of whiskers that are formed at low substrate temperatures where surface deposition is possible but lateral growth is minimized. Coleman and Sears (7) also indicate a situation where “bush” growth of Zn was achieved in a relatively dirty hydrogen environment.

Thus it is demonstrated that the vapor deposited material morphology is affected or potentially modified by the deposition conditions. In general, higher temperature substrate conditions result

in dense, adherent coatings being deposited and as the substrate temperature is decreased the morphology is modified and can become loosely adherent or form non-adherent particles (3). In order to determine what type of trap would be effective to capture the zinc vapor simple test apparatuses were designed and built that could moderate the vaporization temperature and substrate temperature to achieve the desired trapping conditions. These systems were used to determine the effects of inert substrate temperature, filter pore size, and filter temperature on the trapping efficacy.

These experiments were intended to develop a system that could be deployed in the glovebox, the test conditions were limited in scope to those that met the safe design envelop and the size and available utilities. The experimental results and the prototype filter will be described.

## Experimental

Two apparatuses were constructed for these experiments. The first system was comprised of a spherical boiling flask, mantle heater, scroll pump, pressure gauge, thermocouples and temperature controlled glass substrates (Figure 2). The second system was similar to the first except that additional vacuum gauges, a commercial filter holder, and a liquid nitrogen cold trap were incorporated into the system as shown in Figure 3.

Preliminary studies were conducted on the apparatus shown in Figure 2 to determine the effect of temperature on deposit adhesion to an inert substrate. The system was evacuated to a pressure of approximately 30 mTorr, a rate of rise test was conducted, and then the glass fingers were heated to the desired sample deposition temperatures. The thermocouples were monitored and the temperatures were recorded manually. The appearance of the deposit was documented using optical photography and scanning electron microscopy.

Subsequent tests to determine the effect of pore size on trapping efficiency were conducted on the apparatus shown in Figure 3. Commercially available sintered stainless steel filter disks with pore sizes from 0.2  $\mu\text{m}$  to 20  $\mu\text{m}$  were used. The filter disks were 50 mm in diameter and 1.5 mm thick. The filter disks were placed in the filter holder with Teflon gaskets on both sides of the disk and a circumferential Viton O-ring seal was used to maintain vacuum integrity. The system was then evacuated using a scroll pump for an hour prior to heating to the desired temperature. The filter housing was heated about 30 minutes prior to initiating heating of the zinc material to allow for equilibrium temperatures to be achieved prior to exposing the filter to zinc vapors. The mantle surrounding the zinc metal containing flask was then heated to 400°C. This mantle temperature results in an internal temperature of approximately 320°C. Consistent with the vapor pressure curves, it was confirmed that an internal temperature of at least 300°C was required to obtain a reasonable zinc overpressure. The mantle was programmed to hold the temperature for 120 minutes. The internal vessel temperature was reduced to below 280°C prior to cooling the filter. It was desired to maintain the nominal filter deposit temperature as long as the zinc could vaporize. A liquid nitrogen cold trap was used in-line to prevent zinc contamination from fouling the scroll pump. Data were recorded electronically using a Labview data acquisition program for the pressure and temperature. The temperature programmers communicated via RS-232 communication with the computer and data were captured from them as well. The data were then compiled into a single spreadsheet for evaluation.

Tests to determine the effect of filter temperature were conducted using a sintered metal filter disk with a nominal pore diameter of 20 $\mu$ m. This system was evacuated using a scroll pump for at least two hours prior to heating the filter and zinc containing vessel. The data were logged using Labview software and vendor software. The filter heating tape was programmed to heat to the 60, 120, or 200°C set point at a nominal heating rate of 10°C/min and was held for four to five hours. The zinc containing flask was heated 20 minutes after the filter heater to a set point of 400°C at a rate of 10°C / min and was held for 3 hours so a measurable amount of zinc was vaporized for these experiments. The zinc source reached a temperature of 350°C.

The adhesion of the deposit to the filter media was tested using a tape adhesion test; a single roll of tape was used. The samples were weighed, tape was applied to one half of the sample, the tape was removed and the sample reweighed. In addition, the tape was visually examined after removal. The test sequence is shown pictorially in Figure 4. The tape was applied on approximately ½ of the filter and deposit.

The deposit morphology on the half of the sample that was not adhesion tested was examined using scanning electron microscopy. The samples were attached to the SEM stubs and examined at about ¼” from the edge, midway between the center of the sample and the first point and at the center. X-ray dot maps of the elements present were also taken. 5 kV was used for the x-ray analysis and images were taken with accelerating voltages from 5 to 10 kV.

Using these two test techniques the effect of the pore diameter on zinc vapor trapping efficiency and the effect of filter temperature were determined.

## Results and Discussion

The pressure and temperature vs. time profile for the scoping study is shown in Figure 5. The pressure rises significantly after the mantle temperature exceeds 300°C. The typical deposits found on the glass tubes held at the three temperatures are shown in Figure 6 using the test apparatus shown in Figure 2. There is a different deposition density on these samples with the lightest occurring for the lowest temperature and the heaviest for the 100°C sample. The adhesion strength of the samples was not ascertained but the deposit morphology was. The deposits were examined in the SEM with the results shown in Figure 7. It is apparent that a shift in the characteristics occurred over the tested temperature range. The 44 and 100°C samples have flake appearance for the deposit. It is expected that the adherence would not be exceptional for this morphology. The sample held at 225°C shows a regular pattern of crystals with hexagonal and rectangular arrangements apparent.

These results indicate that the higher temperature may increase the likelihood of a better / tighter adherent deposition. The flux may be low enough under these conditions to not form a high density deposit and single fibers and filaments nucleate and grow. The growth is subsequently truncated when new filaments form and grow until they are overtaken by other zinc filaments and islands. No crystallographic analysis was conducted to determine if the hexagonal shapes visible in these images coincide with the basal plane of the HCP zinc.

A typical output from the next series of experiments, using the apparatus shown in Figure 3, is shown in Figure 8 for a 5  $\mu$ m stainless steel filter disk. It takes about 40 minutes for the vessel to

achieve its base pressure. The filter is heated and is held at temperature prior to and for a time slightly longer than the zinc is heated and above 300°C. A small pressure spike is realized when the system is initially heated and this is dissipated until the zinc vessel is heated. Subsequently, the pressure exhibits a more significant peak, it is surmised that this peak represents the release of waters of hydration. The pressure then gradually increases to approximately one Torr during the balance of the experiment. This pressure is in dynamic “equilibrium” between the pump evacuation and the zinc vaporization.

Filter disk samples with varying pore sizes were tested for pump down time and trapping efficiency at a consistent filter temperature of 200°C; a condition selected based on the previous test for the trapping of Zn on the glass fingers and temperature limit for the proposed production facility.

While there was a reduction in the initial pump down rate for the filtered system compared to the baseline system, especially for the filter disks with 0.2 and 1 µm pores, the effect was largely eliminated for filters with nominal pore sizes greater than 1 µm after 1500 seconds. All of the samples achieved approximately the same base pressure. The 0.2 and 1 µm filter samples took slightly longer but after 2000 seconds they were indistinguishable from the other filter media.

The trapping efficiency at 200°C for the various filter media was determined using the mass of the filter. Samples were loaded, evacuated for two hours, then heated to 200°C and held for about an hour prior to heating the zinc source material. The zinc was held above 300°C for approximately 2 hours. The details of the test conditions and the amount of material captured are listed in Table 1. Only single experiments were conducted for all but the 20 µm filters. The results are also presented graphically in Figure 9. There does not appear to be a correlation between zinc capture and pore size. Representative deposits formed on the filters are shown in Figure 10. There are differences in the size of the zinc particles formed on the surface of the filter, but there is no apparent difference in the morphology. Higher magnification images show an open cell structure for the 0.2 as well as the 20 µm filter. Based on these results and the familiarity of the facility with the 20 µm filters, further testing to determine the effects of temperature on trapping were conducted exclusively with the 20 µm filter media.

The mass gains for the 20 µm filters exposed to zinc vapor at the three temperatures are listed in Table 2. These data indicate that more zinc is deposited at the lowest temperature, 60°C. However, this temperature also has the highest loss during the subsequent adhesion testing. The potential transferability of this loosely adherent zinc is a cause for concern for the facility. Thus, higher temperatures are preferred since the zinc appears to be either bound more tightly or captured deeper within the filter media. Figure 11 shows the surface appearance of the filter media for the side facing the zinc vapor. The deposit of zinc near the center of the filter exposed at 60°C is clearly obvious, while deposits at the 120° and 200°C exposures are not. There are also differences in the appearance of the deposit. The 60°C deposit appears like large flakes, Figure 12, while the 120° has both flakes and lacey deposits and the 200°C deposit is predominately lacey. Figure 13 shows the SEM images coupled with Zn X-ray dot maps. These X-ray dot maps clearly show that more zinc is deposited at the lower temperature, however, adhesion testing demonstrated that the deposit is less adherent so this temperature is not recommended.

## Summary and Conclusion

The glass substrate temperature resulted in variations in deposit morphology with lower temperatures exhibiting less organization than higher temperatures. A series of experiments were conducted to define a suitable filter to physically trap zinc vapors that are evolved during a vacuum process. There were no obvious correlations between the filter pore size and the efficacy of zinc vapor trapping, however, the smallest pore sizes had an adverse effect on system evacuation time. While filter media with pore sizes between 5  $\mu\text{m}$  and 20  $\mu\text{m}$  all exhibited similar evacuation times. The 20  $\mu\text{m}$  pore filter media was selected for further testing to determine the effect of temperature on zinc trapping. Filter disks heated to 60°C trapped more zinc than those heated to 120 or 200°C, but this deposit exhibited less adhesion than the higher temperatures. While not fully optimized by the scope of these experiments, a filter disk with a nominal 20 $\mu\text{m}$  pore size heated to 200°C will provide a zinc vapor trap that is effective at reducing the spread of zinc contamination.

## References

1. P. S. Korinko and M.H. Tosten, "Analysis of Zinc 65 Contamination after Vacuum thermal Process", *Journal of Practical Failure Analysis*, Vol. 13, No. 4, 389-395., Aug. 2013.
2. G.W. Sears and J.W. Cahn, "Interaction of Condensable Gases with Cold Surfaces", *J. Chem. Physics*, Vol 33, No. 2, 494-499, 1960.
3. *Physical Vapor Deposition*, T. Parker, Ed., Temescal, 1976.
4. History Of Thin Films Growth, Techniques, Characterization, Péter B. Barna, *Research Institute for Technical Physics and Materials Science of HAS, Budapest, Hungary, Autumn School 2005 on Advanced Materials Science and Electron Microscopy, Humboldt University of Berlin, Oct. 4th - Oct.7th, 2005*.
5. B.A. Movchan and A.V. Demshishin, "Study of the Structure and Properties of Thick Vacuum Condensates of Nickel, Titanium, Tungsten, Aluminum Oxide and Zirconium Dioxide", *Fiz. Metal. Metaloved.*, 28, No. 4, 653-660, 1969.
6. G.W. Sears, "Mechanism of Whisker Growth", *Acta Metallurgica*, Vol 3., 367-369, 1955.
7. R.V. Coleman and G.W. Sears, "Growth of Zinc Whiskers", *Acta Metallurgica*, Vol. 5, 131-136, 1957.
8. J. B. Hudson, "Nucleation of Zinc on Glass", *J. Chem. Physics*, Vol 36, No. 4, 887-889, 1962.
9. M. Kast, P. Schroeder, Y.J. Hyun, P. Pongratz, and H. Bruuckl, "Synthesis of Single Crystal Zn Metal Nanowires using Cold Wall Physical Vapor Deposition", *NanoLetters*, 7, (8), 2540-2544, 2007.

Table 1. Test Condition and results for filters with various pore sizes

Filter	Vessel Temp (°C)	Time T>300°C (s)	Δ mass (mg)	Comments
0.2 μm – 1	333	3965	0.40	Old Config.
20 μm – 4	340	3954	1.31	Old Config.
20 μm – 5	330	4192	1.04	New Config. T varied
0.2 μm – 2	330	7492	2.89	New Config
1 μm – 1	325	7613	1.73	New Config used Zn
5 μm – 1	320	6613	2.57	New Config used Zn
10 μm – 1	324	7689	1.49	New Config used Zn
20 μm – 6	325	7546	1.82	New Config used Zn
20 μm – 7	350	8169	2.14	New Config New Zn
20 μm – 8				

Table 2. Test Condition and results for 20 μm filters held at three temperatures.

Test ID	Vessel T (°C)	Filter A (°C)	Filter B (°C)	Δ mass (mg)	Δ loss ad. (mg)	Comments
60-1	340	55	52	3.8	0.8	Deposit at center
60-3	380	57	50	2.1	0.5	Deposit at center
60-4	384	56	50	3.7	0.5	Deposit at center / Ash on housing
120-2	340	116	96	1.6	0.1	Ash on housing
120-4	384	116	97	2.9	0.2	NA
200-1	340	196	160	2.6	0.3	NA
200-2	340	200	165	5.5*	0.3	Ash on housing
200-4	384	199	149	2.4	0.2	Ash on housing

Notes: “A” refers to thermocouple mounted Above the filter and “B” to the one below. “ad” refers to mass loss during tape adhesion test. \*sample was subjected to a double exposure at 400°C. Missing Test ID are due to poorly executed experiments. The thermocouples were reset on Feb 10, 2011 which resulted in changes in measured vessel temperatures.



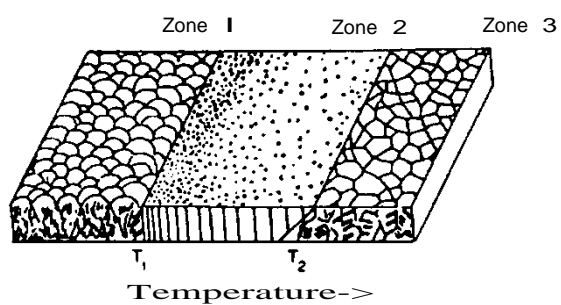
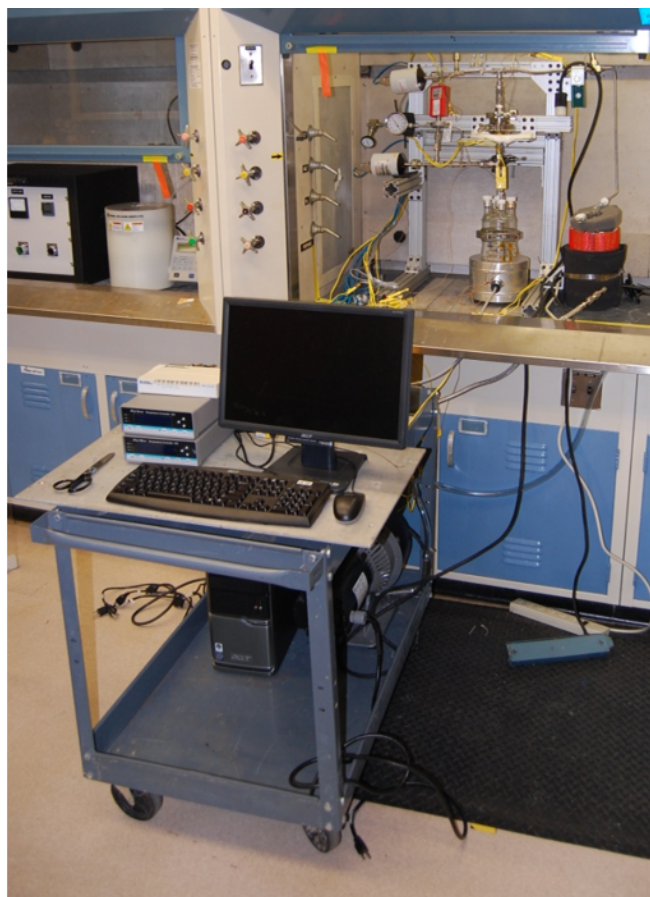


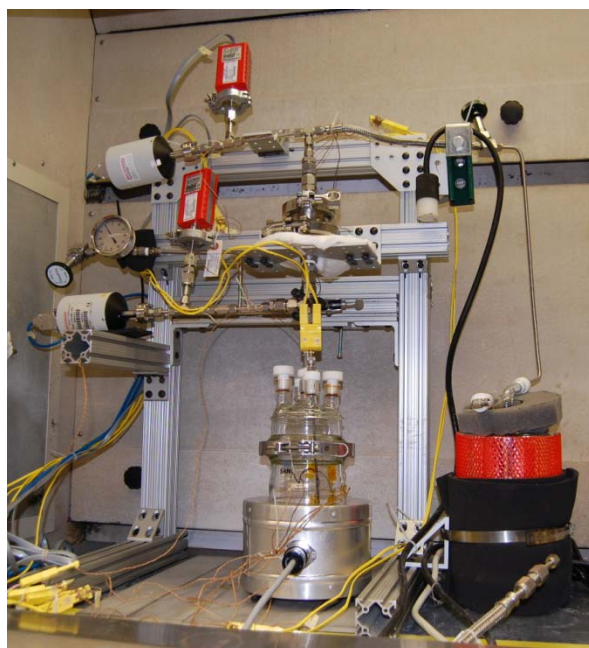
Figure 1. Structural zones in PVD films. From Movchan and Demchishin, Zone 1:  $T < 0.3 T_H$ ; Zone 2:  $0.3 T_H < T < 0.8 T_H$ ; Zone 3:  $T > 0.8 T_H$ , Reference 5.



Figure 2. Screening test apparatus



(a) Complete apparatus computer controller, heater controllers in foreground, system in chemical hood.



(b) Zinc source flask, vacuum gauges, and cold trap



(c) Commercially available filter holder

Figure 3 Second test apparatus assembled for testing filter media.



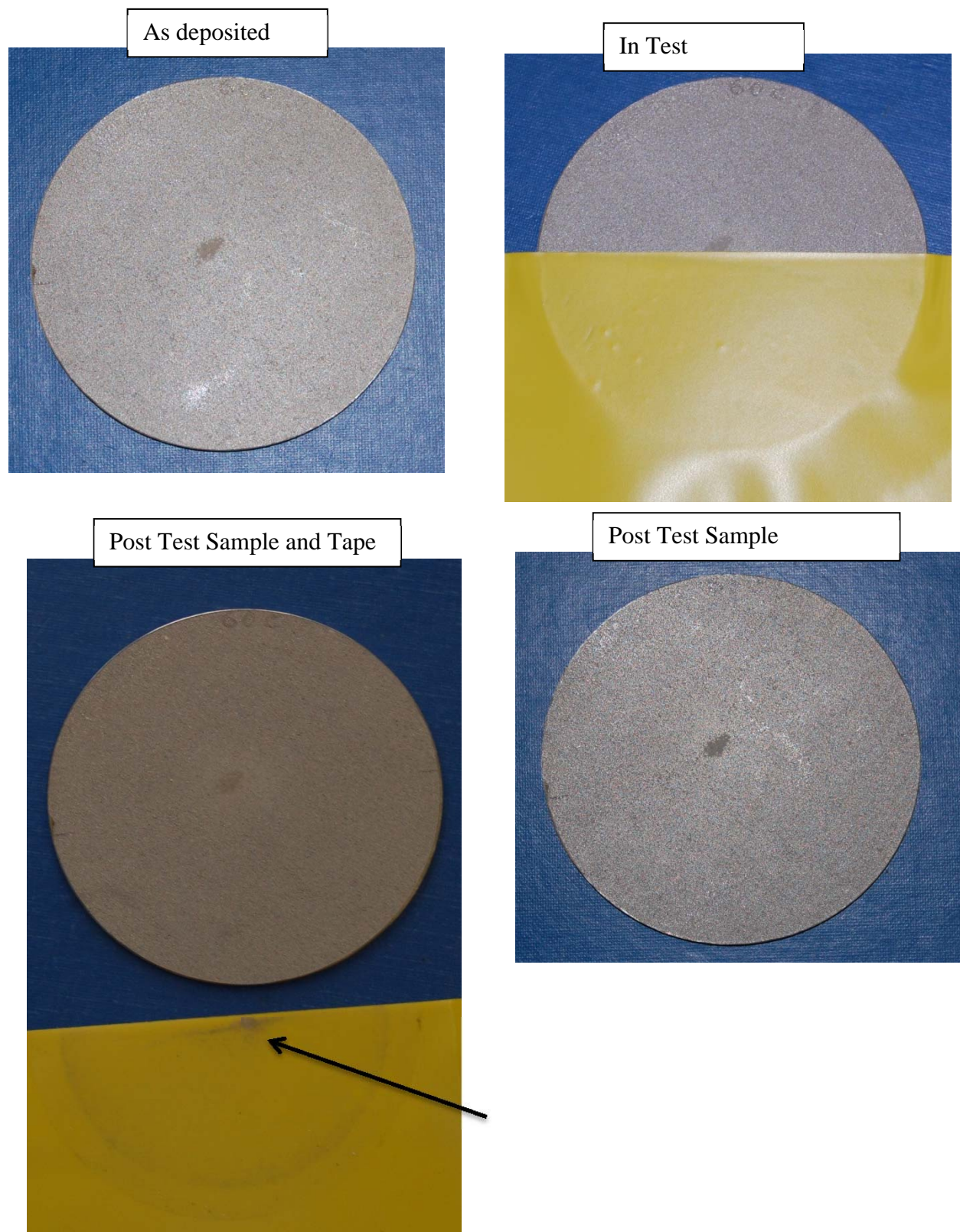


Figure 4. Evolution of adhesion testing using standardized tape, arrow indicates zinc removed from filter disk, (a) as deposited (b) with tape applied (c) filter disk and tape (d) filter disk.

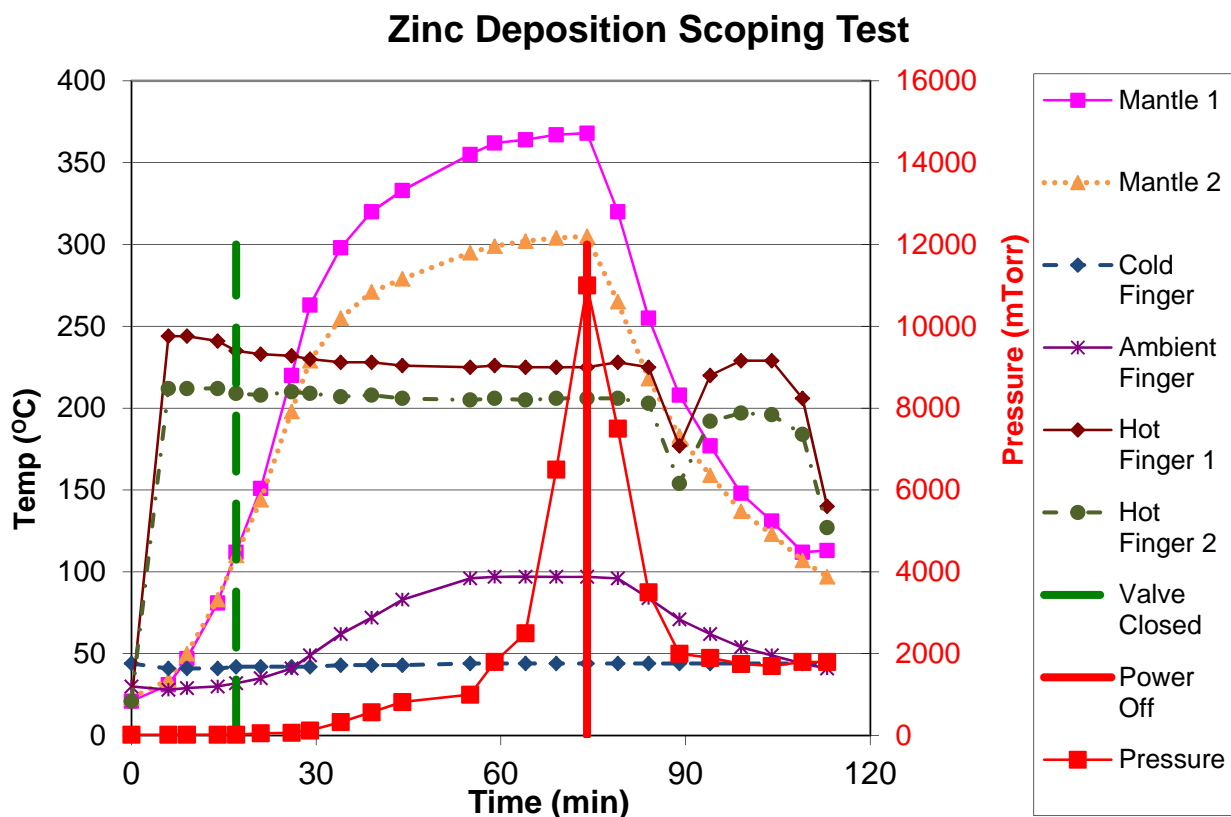


Figure 5. Thermal and pressure profile for scoping test.



(a) 44°C

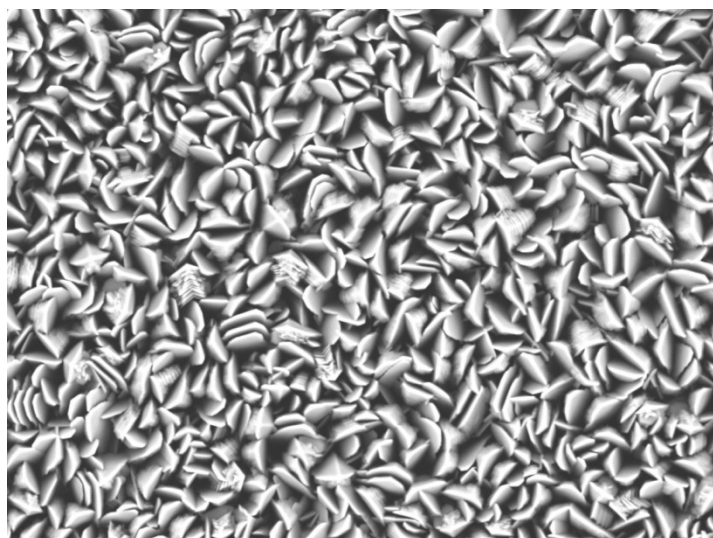


(b) 100°C



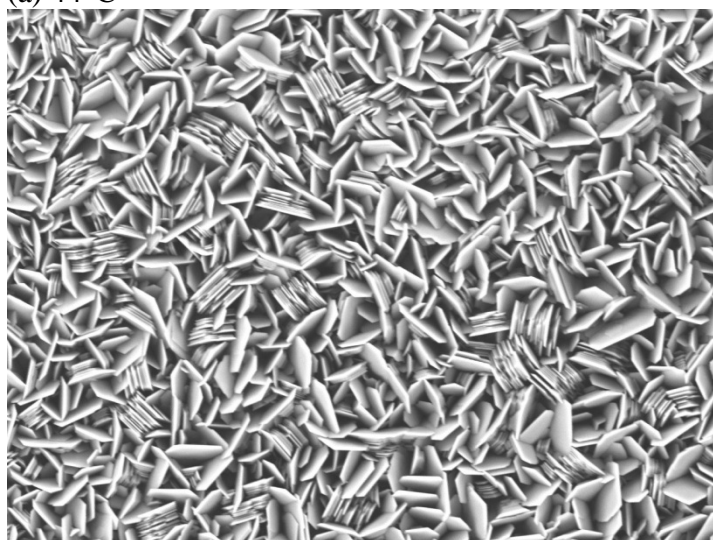
(c) 225°C

Figure 6. Deposits formed on Pyrex glass tubes held at (a) 44°C, (b) 100°C, and (c) 225°C.



2009/03/16 14:02 D1.9 30 um

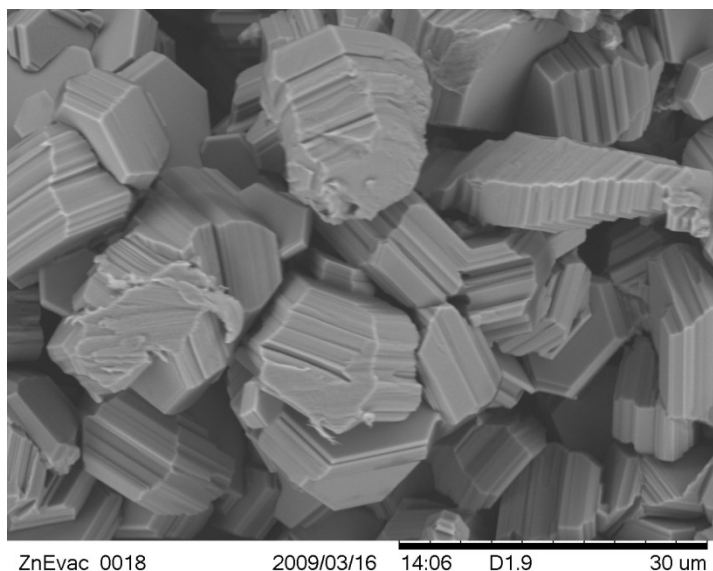
(a) 44°C



2009/03/16 13:57 D1.9 30 um

(b) 100°C





(c) 225°C

Figure 7. SEM images of the deposit morphology from the tubes shown in Figure 6, (a) 44°C, (b) 100°C, and (c) 225°C.

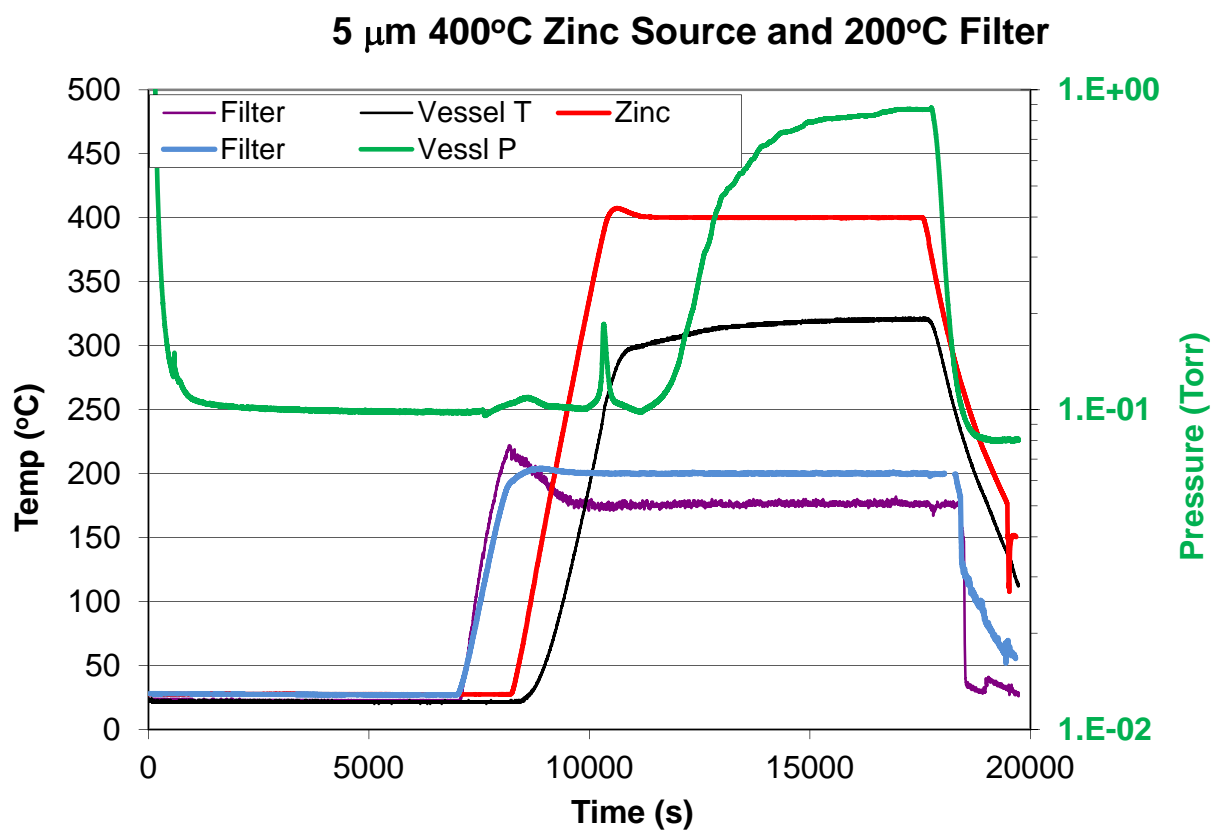


Figure 8. Typical thermal and pressure response for a 5  $\mu\text{m}$  filter.



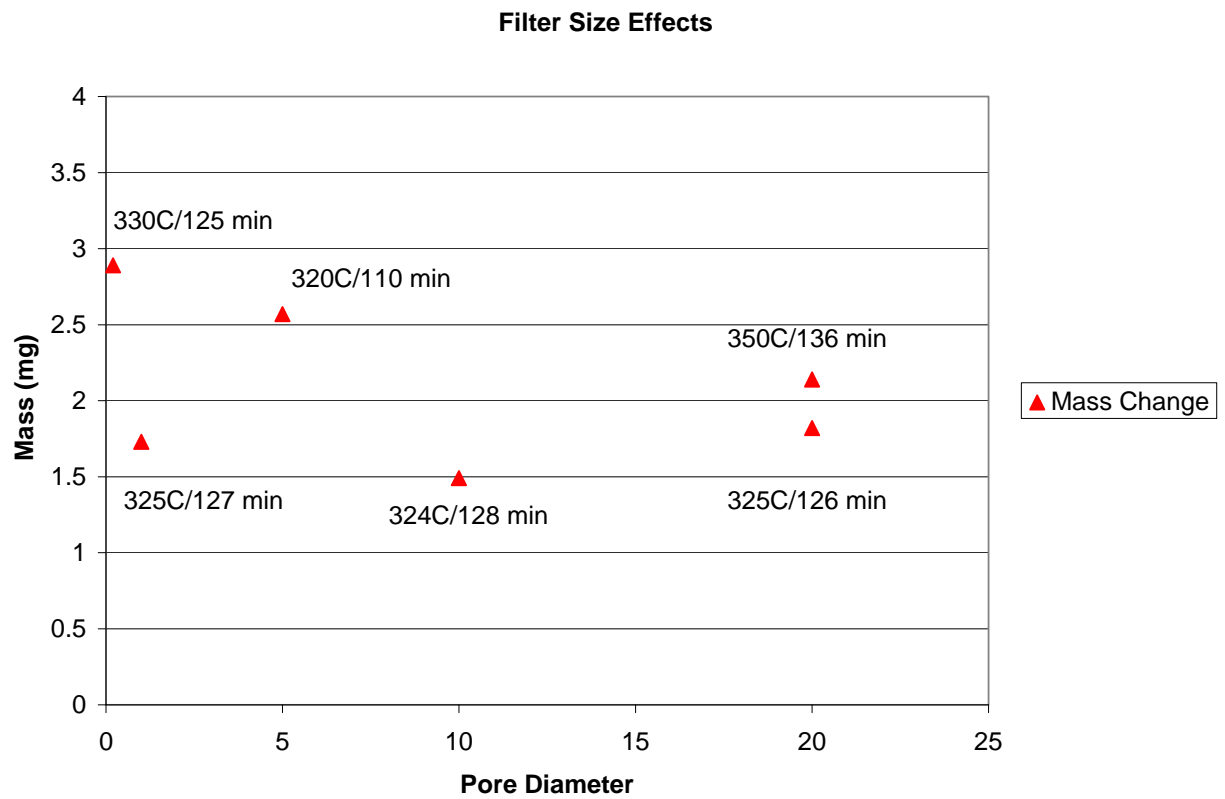
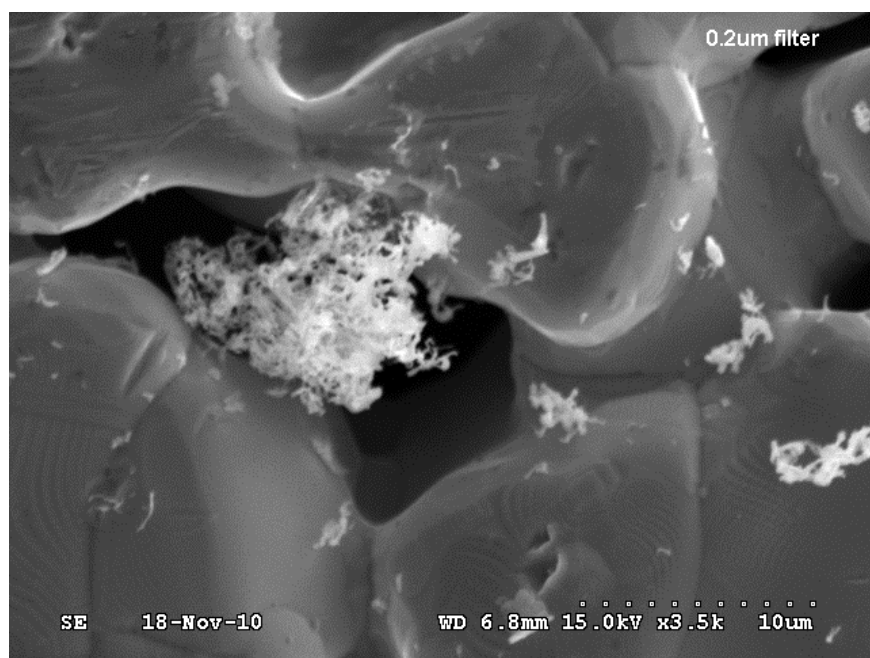
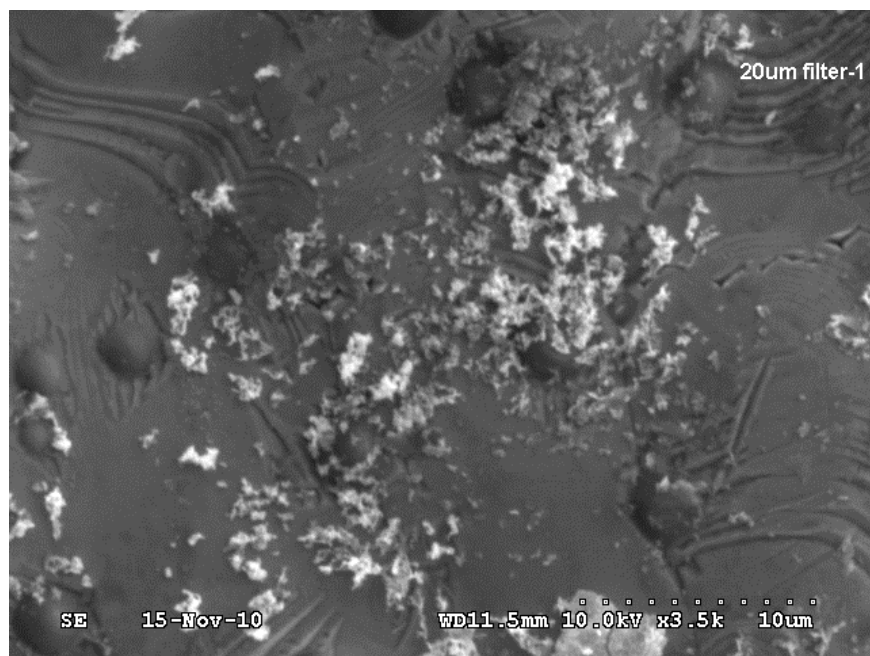


Figure 9. Mass gain results for filters heated to 200°C with pore sizes from 0.2 to 20 μm.



(a) 0.2  $\mu\text{m}$  pore size



(b) 20  $\mu\text{m}$

Figure 10. Zn deposit structure on the center of the (a) 0.2 and (b) 20  $\mu\text{m}$  pore size filter disk.

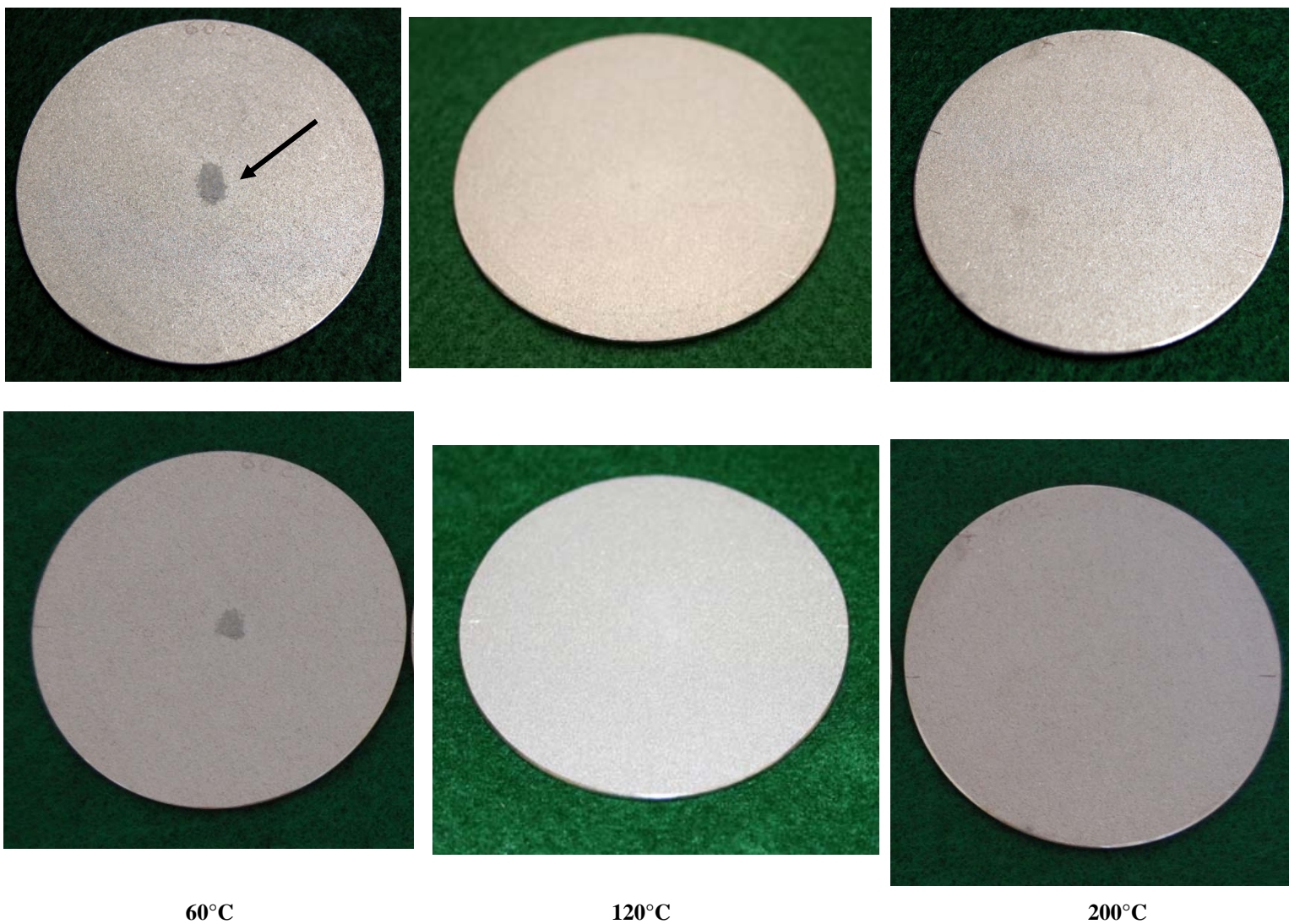
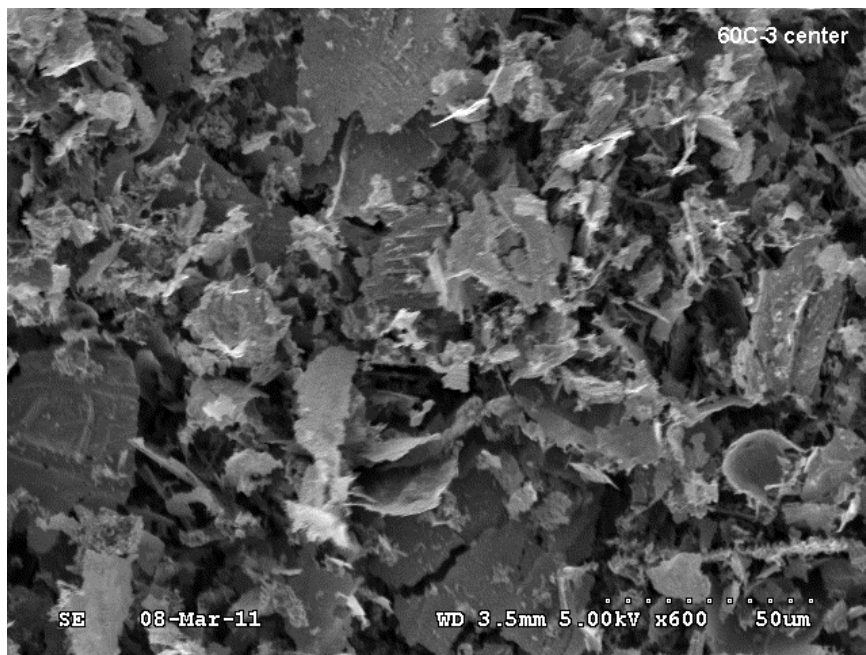
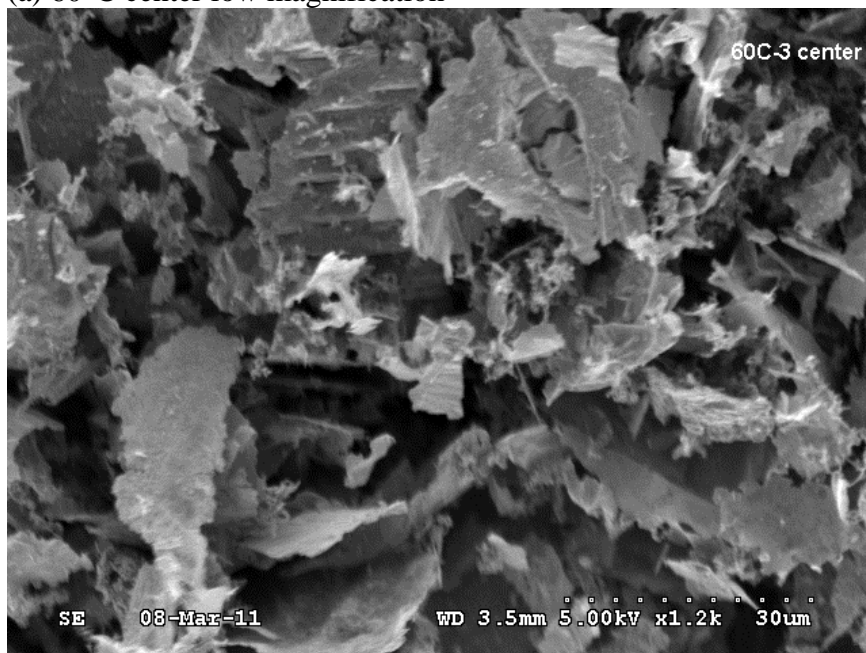


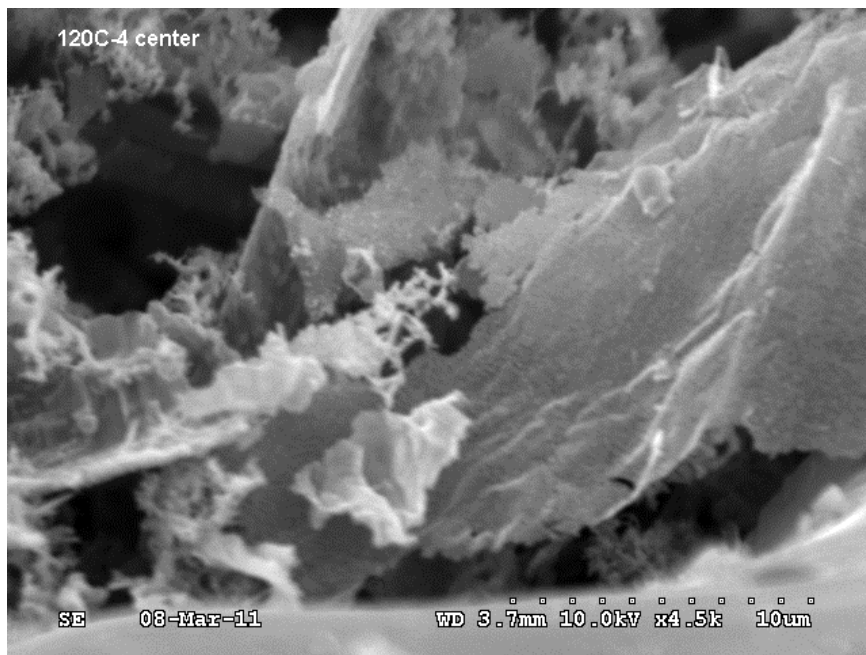
**Figure 11. Deposit appearance for filters exposed at 60°C, 120°C, and 200°C in the as deposited (upper) and adhesion tested (lower) conditions. Note: about half the deposit was removed from the 60°C sample. This result was consistent across all three 60°C filter exposures.**



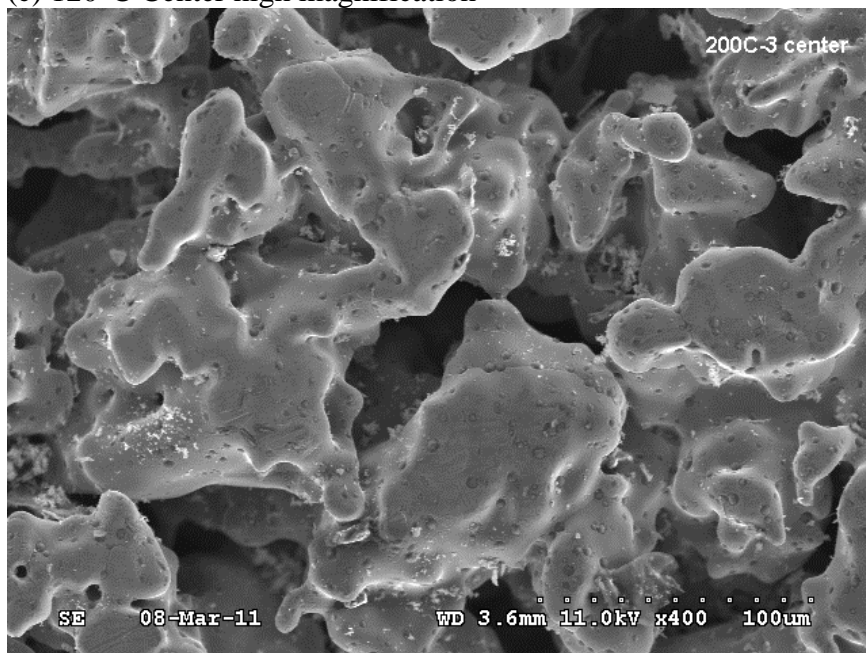
(a) 60°C center low magnification



(b) 60°C Center higher magnification

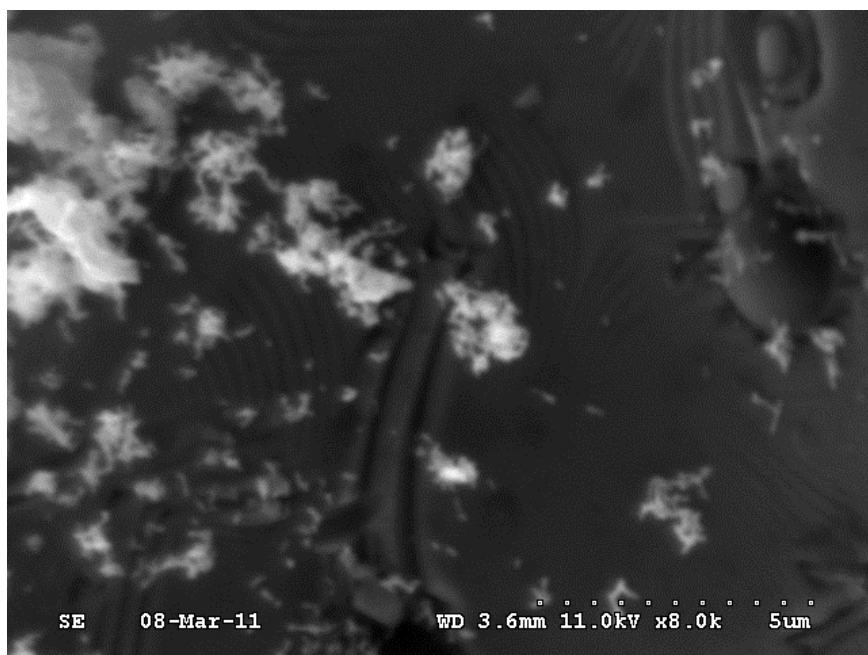


(c) 120°C Center high magnification



(d) 200°C Center low magnification





(e) 200°C Center high magnification

Figure 12. SEM images of the deposits taken near the center of the filter after exposure at (a) 60°C low magnification (b) 60°C high magnification (c) 120°C high magnification, (d) 200°C low magnification and (e) 200°C high magnification. Note the changes in deposit from flaky to lacey as the temperature increases.

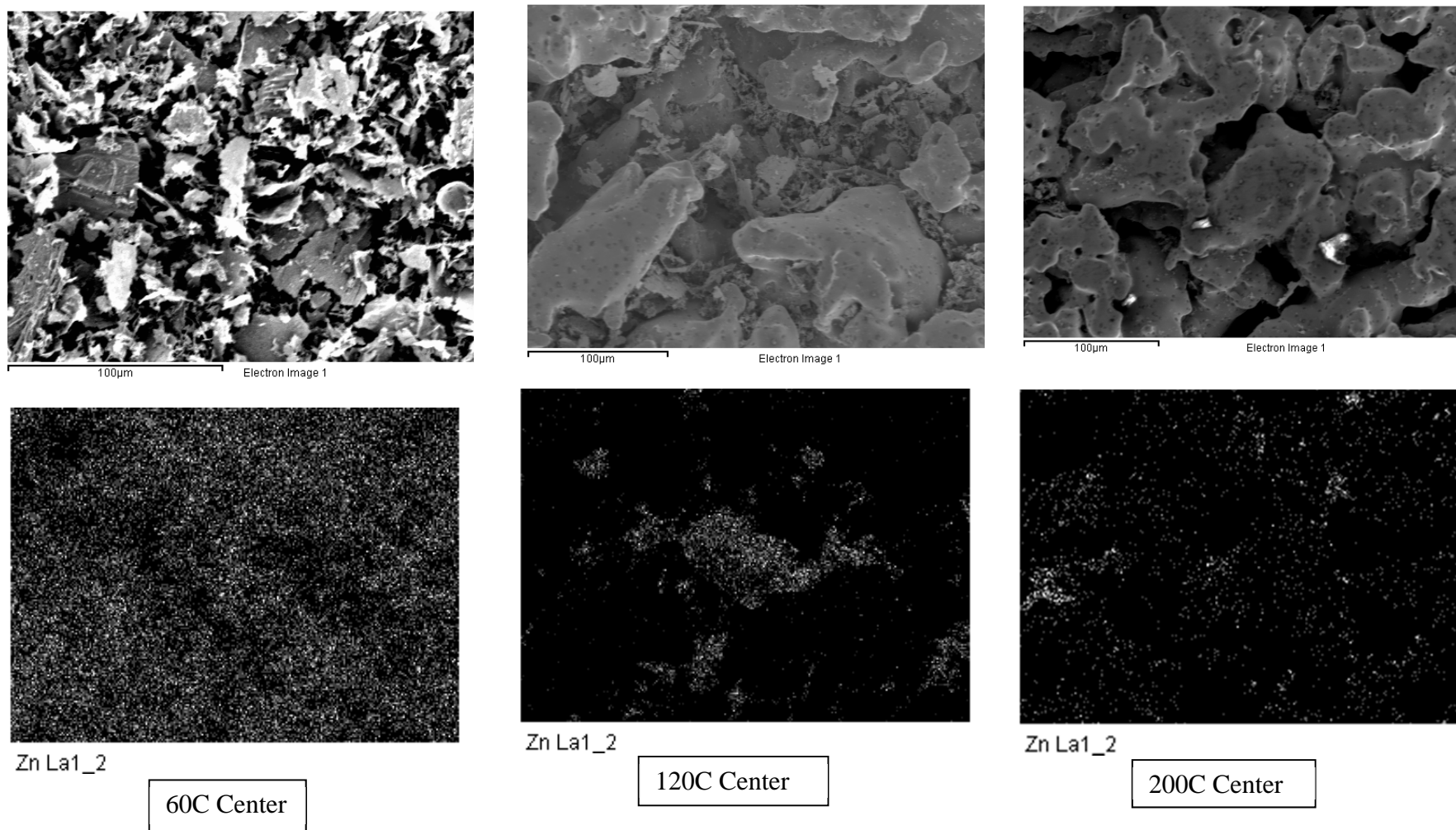


Figure 13. SEM images and X-ray dot maps of the filter disks after exposure, the dot density indicates the amount and location of the zinc deposit (a) 60°C SEM (b) 60°C X-ray dot map (c) 120°C SEM (d) 120°C X-ray dot map (e) 200°C SEM (f) 200°C X-ray dot map.